New Phytologist

Research

Catechol, a major component of smoke, influences primary root growth and root hair elongation through reactive oxygen species-mediated redox signaling

Ming Wang[1], Matthias Schoettner[1], Shuqing Xu[1], Christian Paetz[2], Julia Wilde[1], Ian T. Baldwin[1] and Karin Groten[1]

[1]Department of Molecular Ecology, Max Planck Institute for Chemical Ecology, Hans-Knoell-Str. 8, 07745 Jena, Germany; [2]NMR Group, Max Planck Institute for Chemical Ecology, Hans-Knoell-Str. 8, 07745 Jena, Germany

Author for correspondence:
Karin Groten
Tel: +49 3641 571000
Email: kgroten@ice.mpg.de

Received: *3 May 2016*
Accepted: *29 September 2016*

New Phytologist (2017) **213:** 1755–1770
doi: 10.1111/nph.14317

Key words: antioxidant, auxin, catechol, *Nicotiana attenuata*, post-fire annual, reactive oxygen species (ROS), smoke.

Summary

- *Nicotiana attenuata* germinates from long-lived seedbanks in native soils after fires. Although smoke signals have been known to break seed dormancy, whether they also affect seedling establishment and root development remains unclear.
- In order to test this, seedlings were treated with smoke solutions. Seedlings responded in a dose-dependent manner with significantly increased primary root lengths, due mainly to longitudinal cell elongation, increased numbers of lateral roots and impaired root hair development. Bioassay-driven fractionations and NMR were used to identify catechol as the main active compound for the smoke-induced root phenotype.
- The transcriptome analysis revealed that mainly genes related to auxin biosynthesis and redox homeostasis were altered after catechol treatment. However, histochemical analyses of reactive oxygen species (ROS) and the inability of auxin applications to rescue the phenotype clearly indicated that highly localized changes in the root's redox-status, rather than in levels of auxin, are the primary effector. Moreover, H_2O_2 application rescued the phenotype in a dose-dependent manner.
- Chemical cues in smoke not only initiate seed germination, but also influence seedling root growth; understanding how these cues work provides new insights into the molecular mechanisms by which plants adapt to post-fire environments.

Introduction

Fire is a predictably irregular natural event in many regions of the world; fire frees up space, nutrients and light, allowing seedlings to become established (Rundel, 1981; Baldwin *et al.*, 1994; Nelson *et al.*, 2009). Regrowth, reproduction and germination are synchronized in the immediate post-fire environment. Some plant species are classified as fire ephemerals, which germinate synchronously only after fires that start in long-lived seedbanks in the soil (Keeley & Pizzorno, 1986; Baldwin & Morse, 1994; Preston & Baldwin, 1999). One of the key compounds of smoke that promotes seed germination and is required for synchronizing mass germination after fire has been identified as 3-methyl-2H-furo[2,3-c]-pyran-2-one, also known as karrikin1 (KAR1) (Flematti *et al.*, 2004a,b); by contrast, catechol, a major constituent in smoke, does not induce germination (Baldwin *et al.*, 1994). Catechol is known to interact with both organic compounds (e.g. amino acids) and inorganic compounds (e.g. metal ions) (Yang *et al.*, 2014), and has a complex redox chemistry in the presence of metal ions (Schweigert *et al.*, 2001).

Treatments with smoke water and smoke extracts not only induce germination, but also enhance root growth in rice (Kulkarni *et al.*, 2006), tomato (Taylor & Van Staden, 1998), jatropha (Abdelgadir *et al.*, 2012), rapeseed (Abdollahi, 2012), papaya (Chumpookam *et al.*, 2012) and maize (Soós *et al.*, 2009). However, for most of this work, it is not clear which compound(s) in smoke is(are) responsible for the improved growth and how the signals that result in growth promotion are transduced into cellular processes.

Primary root growth requires two main physiological processes: the proliferation of daughter cells in the apical meristem and the enlargement of differentiated cells that are no longer in the meristem. When cells stop expanding, they are considered morphologically to belong to the mature zone, which is characterized by root hair development and vascular tissue formation (Petricka *et al.*, 2012). All of these developmental processes are regulated by different plant hormones, among which auxins are the best studied (Sabatini *et al.*, 1999; Galinha *et al.*, 2007; Dinneny & Benfey, 2008). That the control of auxin biosynthesis and signaling is important for root growth and development has been shown by external applications of auxins, which result in increased cell

division but decreased root growth in Arabidopsis (Rahman *et al.*, 2007; Zhou *et al.*, 2011), whereas the addition of auxin biosynthesis inhibitors, L-kynurenine (Kyn) (He *et al.*, 2011) and yucasin (Nishimura *et al.*, 2014) leads to increased primary root growth. Auxin gradients are also regulated by transport systems (Tromas & Perrot-Rechenmann, 2010; Zhou *et al.*, 2011; Adamowski & Friml, 2015; Draelants *et al.*, 2015; Rodríguez-Sanz *et al.*, 2015). Furthermore, among other factors, auxin-regulated gene expression is controlled by the *SHY2* (short hypocotyl) gene encoding IAA3, a member of the Aux/IAA family (Tian *et al.*, 2002).

In addition to auxin, reactive oxygen species (ROS) are important signaling molecules that play a role not only in plants' responses to biotic and abiotic stress, but also in plant growth and development (Gapper & Dolan, 2006; Petrov & Van Breusegem, 2012; Foyer & Noctor, 2013). *In planta*, O_2^- is produced by NADPH oxidases (RBOH) and can be further converted into H_2O_2 by superoxide dismutases (SODs) and other enzymes, including apoplastic oxalate oxidase, diamine oxidase and class III peroxidases. H_2O_2 can be catabolized enzymatically to H_2O by catalase (CAT), glutathione peroxidase (GPX) and ascorbate peroxidase (APX) or it can be consumed nonenzymatically by Fenton reactions when Fe^{2+} is available; such a reaction depends greatly on pH and other indicators of subcellular reactivity. As demonstrated by mutants, the main ROS appear to have different zones of accumulation within roots, and their generation and balance is controlled by the bHLH transcription factor UPBEAT; superoxide accumulates in the meristematic zone, whereas H_2O_2 accumulates in the elongation/differentiation zone (Tsukagoshi *et al.*, 2010). Furthermore, the presence and localization of ROS in the growing root hair, in particular the root tip, is decisive for the growth of the hair, and Arabidopsis RBOHC mutants impaired in H_2O_2 production are defective in root hair elongation (Foreman *et al.*, 2003).

The cell wall plays an important role in cell expansion, and the primary cell walls are composed primarily of microfibrils, hemicelluloses, pectins and structural proteins such as hydroxyproline-rich O-glycoprotein extensins (EXT) (Velasquez *et al.*, 2011; Nguema-Ona *et al.*, 2014; Xiong *et al.*, 2015). ROS can contribute to the tightening and the loosening of cell walls. Cell-wall tightening is assumed to be due to the cross-linking of cell-wall components. This process is concentration-dependent: moderate levels of H_2O_2 and proper cross-linking are essential for root growth, whereas excessive levels of H_2O_2 dramatically inhibit cell expansion and may be directly toxic, oxidizing DNA, proteins and metabolites (Tenhaken, 2014; Kärkönen & Kuchitsu, 2015). Cell-wall loosening and underlying root elongation were suggested to be at least partly due to the production of the hydroxyl radical; this radical can be produced from H_2O_2 in the presence of metal ions through the Fenton reaction (Liszkay *et al.*, 2004) and leads to the cleavage of cell-wall polysaccharides (Fry *et al.*, 2001; Carol & Dolan, 2006; Kim *et al.*, 2014).

At the molecular level, members of the receptor-like kinase CrRLK1 family have been shown to control cell wall properties and cell expansion (Anders *et al.*, 2014), and in Arabidopsis, MED25/PFT1 has been reported as a mediator that controls root hair differentiation and primary root elongation by regulating the expression of several genes encoding redox-active proteins; the expression of these genes critically alters the balance of H_2O_2 and O_2^- (Sundaravelpandian *et al.*, 2013; Raya-González *et al.*, 2014).

Nicotiana attenuata, or wild tobacco, is a summer annual native to the Great Basin desert of California, Nevada, Idaho and Utah, USA; it primarily occurs ephemerally for up to three growing seasons after wildfires and persistently in certain areas that do not accumulate leaf litter (Goodspeed, 1955; Preston & Baldwin, 1999). As a fire-chasing species, *N. attenuata* seed germination after fires has been studied extensively (Baldwin & Morse, 1994; Baldwin *et al.*, 1994), and a wealth of ecological and molecular knowledge is available for this species. However, surprisingly, little is known about the additional effects of smoke on the establishment of seedlings and their root growth in the post-fire habitat.

Here we tested the hypothesis that smoke has additional effects on the growth of *N. attenuata* seedlings with a root morphology-guided approach. We identified catechol as the main active compound in smoke which shapes root architecture in a dose-dependent manner. Histological, transcriptome and analytical results provide evidence that ROS, and not auxin, are the primary regulators of the catechol-induced root phenotype; the phenotype results from alterations in ROS homeostasis in the root cortex of the elongation zone, in root hairs and within the roots.

Materials and Methods

Plant material and growth

In all experiments, wild-type *Nicotiana attenuata* Torr. Ex Watts seeds of the 31st generation inbred line were used. Seed germination and plant growth were performed as described (Kruegel *et al.*, 2002). In brief, seeds were sterilized and germinated on agar with Gamborg B5 (Duchefa, The Netherlands, http://www.duchefa.com) after soaking for 1 h in a 1 : 50 (v/v) diluted liquid smoke (House of Herbs, Passaic, NY, USA) supplemented with 1 mM of gibberellic acid (GA_3). Seedlings were grown vertically in Percival chambers (Perry, IA, USA) at 28°C, under long-day conditions (16 h : 8 h, light : dark). Seedlings were either directly germinated on the supplemented media (long-term treatment) or transferred 5 d post-germination (dpg) to the supplemented media (short-term treatment). For the long-term treatment (13 dpg, data for Fig. 1), liquid smoke was added to the GB5 medium before autoclaving. For all other short-term treatments, the chemicals were added to cooled GB5 media (*c.* 45–50°C), using the concentrations indicated in the text and figures, and seedlings were phenotyped hours or days after treatment.

Chemicals and stock solutions

Stock solution were prepared and filtered with 22-nm sterilized filters: Indole-3-acetic acid (IAA, CAS-no. 87-51-4, Duchefa, https://www.duchefa-biochemie.com/, dissolved in ethanol), 1-naphthaleneacetic acid (NAA, CAS-no. 86-87-3, dissolved in 1 M NaOH), N-1-naphthylphthalamidic acid (NPA, CAS-no. 132-66-1, Santa Cruz Biotechnology, dissolved in DMSO), L-kynurenine (Kyn, CAS-no. 2922-83-0,

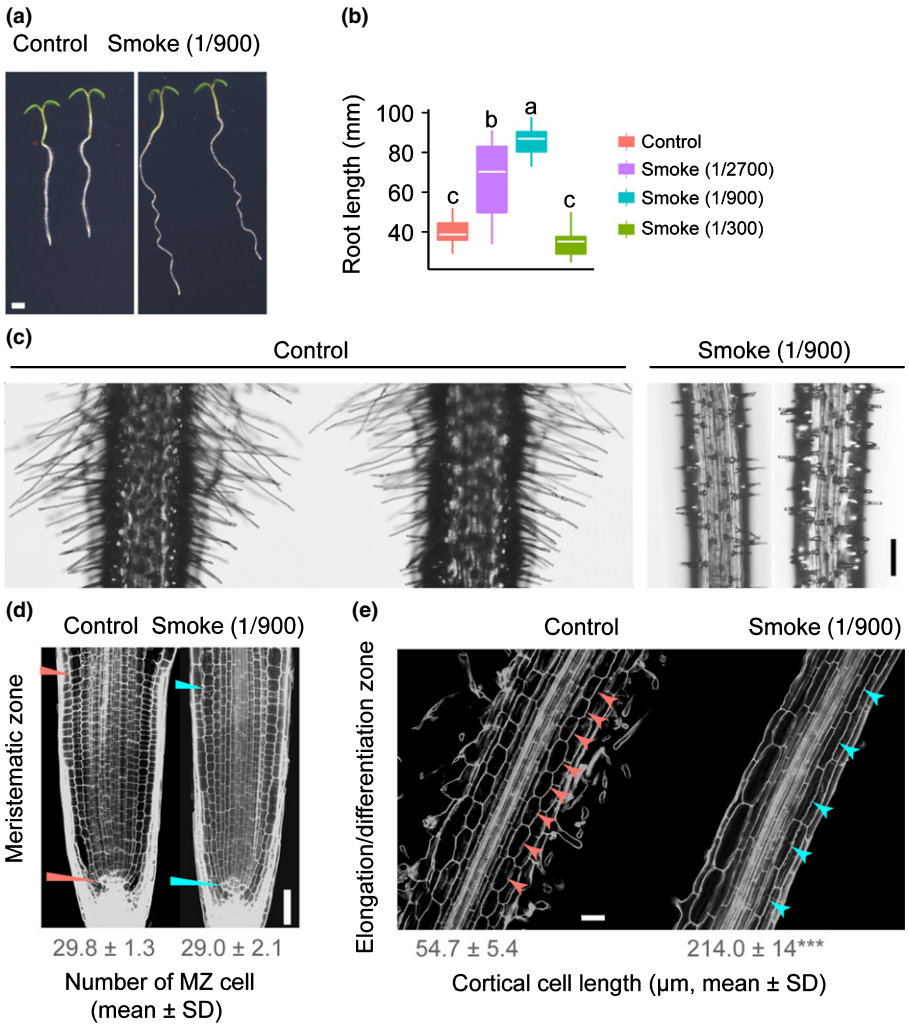

Fig. 1 Treatment of *Nicotiana attenuata* seedlings with liquid smoke increases primary root growth and decreases root hair elongation. Root phenotype is induced by smoke treatment. *Nicotiana attenuata* seedlings were germinated on GB5 medium containing liquid smoke (v/v = 1/900) and compared to mock-treated roots. Measurements were taken 13 d post-germination (dpg). (a) A scan of seedlings revealed the increase in primary root length after smoke treatment. Bar, 0.2 mm. (b) The effect of smoke treatment is concentration-dependent ($n = 6$, for each biological replicate 25–30 seedlings per Petri dish were measured); different letters indicate significant differences ($P \leq 0.05$, one-way ANOVA followed by Tukey's HSD), box plots show the medium (white horizontal line), the upper and lower quartile (upper and lower end of the box) and the minimum and maximum (whiskers). (c) Root hair phenotype was observed by Zeiss ApoTome imaging under bright-field. Bar, 10 µm. (d, e) Confocal microscope imaging after propidium iodide (PI) staining to visualize the cell walls. Bars, 50 µm. (d) The number of meristem cells did not change after smoke treatment. The distances of meristem zone (MZ; left half only) for measuring are marked by arrow-heads. (e) After smoke treatment, cells in the elongation zone were significantly longer than cells in the elongation zone of controls. Only cells in the cortex layer were measured (see also Supporting Information Fig. S2). A representative picture of the elongation/differentiation zones (EZ/DZ) is shown. The arrowheads point to the elongated cells. Data are means ± SD (20–25 seedlings were measured), significant differences are indicated by asterisks (Student's *t*-test: ***, $P \leq 0.001$) (see also Fig. S1).

Sigma-Aldrich, dissolved in DMSO), 5-(4-chlorophenyl)-4H-1,2,4-triazole-3-thiol (yucasin, CAS-no. 26028-65-9, Sigma-Aldrich, dissolved in DMSO), diphenyleneiodonium chloride (DPI, CAS-no. 4673-26-1, Sigma-Aldrich, dissolved in DMSO), BES-H_2O_2-AC (WAKO, www.wako-chem.co.jp/english/labchem/, dissolved in DMSO), 1,2-dihydroxybenzene (catechol, CAS-no. 120-80-9, Sigma-Aldrich, dissolved in 80% methanol), 1,3-dihydroxybenzene (resorcinol, CAS-no. 108-46-3, Sigma-Aldrich, dissolved in 80% methanol), 1,4-dihydroxybenzene (hydroquinone, CAS-no. 123-31-9, Sigma-Aldrich, dissolved in 80% methanol), 2-methoxyphenol (guaiacol, CAS-no. 90-05-1, Sigma-Aldrich, dissolved in 80% methanol) and nitro blue tetrazolium (NBT, CAS-no. 298-83-9, Sigma-Aldrich, in 20 mM phosphate buffer pH 6.1).

Phenotyping experiments

In order to determine the length of primary roots, pictures of seedlings were scanned using a desktop scanner at 600 dpi. These scanned pictures were further measured using ImageJ (NIH). For root hair phenotyping, macro-images were taken under a stereomicroscope (MZ16, Leica, Wetzlar, Germany) and micro-images were taken by ApoTome (Zeiss, Oberkochem, Germany) microscope.

Extraction, fractionation and purification of liquid smoke and burnt soil

Solid phase extraction (Multi 96 HR-XC (96 × 25 mg) column (Macherey Nagel, Düren, Germany) was used as first step of liquid smoke fractionation to isolate the active compound. In brief, 0.8 ml undiluted liquid smoke (House of Herbs, Passaic, NY, USA) was loaded onto an activated column and flow-through was collected as S0, then successively eluted with 1 ml each of 1 M HCOOH, 80% methanol in HCOOH, 100% methanol, 0.35 M NH_4OH, 0.35 M NH_4OH in 60% methanol and 2 M NH_4OH in acetone. At each step the eluted flow-through was collected and desiccated as S0–S6 fractions, dissolved eventually in methanol and the obtained fractions used for further bio-assay and high power liquid chromatography (HPLC) fractionation. A detailed description of HPLC fractionation, mass acquisition by UPLC/electrospray ionization-time of flight (ESI-TOF) and catechol quantification is provided in the Supporting Information Methods S1.

Soil was collected from a burn in 2016 from the native habitat of *N. attenuata* in Arizona, USA. Milled soil was dissolved in methanol (80%) and analyzed after solid phase extraction. The same method was employed for catechol quantification as already described. Catechol content was measured by UPLC/ESI-qTOF with the standard curve method.

Structure elucidation by NMR

Collected fractions were dried completely in a vacuum concentrator (3.7 mbar, Concentrator 5301, Eppendorf). The merged active HPLC-fractions 'd3' and 'd4' were used for structure elucidation by nuclear magnetic resonance spectroscopy (NMR). ^{1}H NMR, ^{13}C NMR and ^{1}H-^{13}CHSQC spectra were recorded on an Avance500 NMR spectrometer (Bruker-Biospin, Karlsruhe, Germany) at 300 K using a 5 mm TCI CryoProbe™. Chemical shift values (δ) are given relative to the residual solvent peaks at δ_H 3.31 and δ_C 49.05, respectively. Coupling constants are given in hertz (Hz).

RNA isolation

For our large-scale gene expression analysis, roots were treated with the S2 fraction or the same amount of methanol as a control. Root tips were harvested 2 and 6 h after treatment. At least 200 seedlings were harvested as one replicate and kept in RNAlater (Qiagen, https://www.qiagen.com/de/) until being extracted. In total, three replicates per time-point and treatment were harvested. RNA was extracted using Qiagen RNeasy Mini Kit columns (Qiagen) according to manufacturer's protocols, in combination with on-column DNase-I treatment (Qiagen). Aliquots (1 µl) of purified RNA were pipetted for quantification and quality assessment of total RNA using the Agilent 2100 Bioanalyser system in combination with RNA 6000 n kit (Agilent, Santa Clara, CA, USA). Only RNA that displayed intact 18S and 25S peaks was sent for RNA-seq profiling (Max Planck Genome Centre Cologne, Germany). All libraries were sequenced on the Illumina HiSeq 3000 (Illumina, https://www.illumina.com/).

RNA-seq data analysis

For data analysis, we followed the descriptions of Ling *et al.* (2015). Briefly, the raw reads were trimmed with ADAPTERREMOVAL (Lindgreen, 2012), which were subsequently aligned to the *N. attenuata* genome assembly (release 1.0) using TOPHAT2 (Kim *et al.*, 2013). The genes were assembled by CUFFLINKS in combination with *N. attenuata* genome annotation as the reference. Re-mapping all trimmed reads to the assembled transcripts via RSEM was used to estimate the expression level of the assembled transcripts. Read count were calculated using HT-SEQ (Anders *et al.*, 2014) using *N. attenuata* genome annotation. The trimmed mean of M-values (TMM) normalized fragment per kb of transcript per million mapped reads (FPKM) was calculated using TRINITY (Haas *et al.*, 2013). The differentially expressed genes (DEG) were identified using EDGER package (Grman & Robinson, 2013). Genes with the absolute fold-change of > 2 and with a false discovery rate (FDR)-adjusted *P*-value of < 0.05 were considered as differentially expressed genes (DEGs). The gene ontology (GO) annotations of *N. attenuata* genes were derived from its genome annotation (S. Xu, T. Brockmöller, A. Navarro-Quezada, H. Kuhl, K. Gase, Z. Ling, W. Zhou, C. Kreitzer, M. Stanke, H. Tang, E. Lyons, P. Pandey, S. P. Pandey, B. Timmermann, E. Gaquerel & I. T. Baldwin, upublished). The functional enrichment analysis was computed by CLUGO. The levels of significance of enriched GO terms were determined by Bonferroni corrected *P*-values ($P \leq 0.05$).

Indole-3-acetic acid (IAA) extraction and measurement

Root and leaf tissues were separated, and roots dissected after long-term treatment with smoke (5 dpg) and short-term treatment with catechol (48 h) and immediately frozen in liquid nitrogen. After being ground to a fine power, IAA was extracted and concentration was determined as described in detail by Schaefer *et al.* (2016). In brief, total IAA was extracted with extraction buffer (methanol : 1 M formic acid = 4 : 1 (v/v)), and IAA was measured relative to labeled D-IAA by a Bruker Elite EvoQ Triple quad-MS equipped with a HESI (heated electrospray ionization) ion source (Bruker Daltonik, Bremen, Germany).

Superoxide anion (O_2^-) and hydrogen peroxide (H_2O_2) staining and quantification

Seedlings grown on GB5 media were transferred to media supplemented with smoke, catechol, and inhibitors of ROS and H_2O_2 for the indicated time-points. For superoxide anion staining with NBT, seedlings were stained for 15 min in a solution of 2 mM NBT in 20 mM phosphate buffer (pH 6.1). Transferring stained seedlings into distilled water stopped the reaction. Pictures were taken by Leica stereomicroscope (MZ16, Leica, Wetzlar, Germany). Settings were exactly identical for all of the pictures in the same experiment. To visualize H_2O_2, seedlings were incubated in 50 µM BES-H_2O_2-AC for 30 min in the dark; and for the simultaneous visualization of H_2O_2 and plant cell walls in a single specimen, seedlings were double-stained by

incubation in 100 μM of propidium iodide (PI) and 50 μM of BES-H_2O_2-AC for 30 min in the dark. After three quick rinses, pictures were immediately taken by LSM 510 (Zeiss, Jena, Germany). The excitation wavelength for PI-stained samples was 536 nm, and emission was collected at 617 nm; for BES-H_2O_2-AC stained samples excitation was 485 ± 20 nm, and emission collected at 515 ± 20 nm. For imaging after NBT and BES-H_2O_2-AC staining, all of the instrumental parameters were retained in an independent experiment.

ImageJ software (NIH, https://imagej.nih.gov/ij/) was used to assess the average intensity of NBT-stained signals and the relative amount of H_2O_2 fluorescence intensity by BES-H_2O_2-AC. Briefly, original captured images were loaded and inverted to 8-bit mode, and then the images were processed under the menu of 'Process' to subtract background, followed by calibration under the menu of 'Analyze', the default value of the threshold of 'Adjust' was kept for measuring the next step. All of the 'IntDen' values were exported to Microsoft Excel for statistical analysis.

The H_2O_2 content of the roots after staining with BES-H_2O_2-AC staining was analyzed by Amplex Red hydrogen peroxide/peroxidase assay kit (Thermo Fisher Scientific, https://www.thermofisher.com, USA) according to the manufacturer's instruction. Briefly, six root sections of 1–1.5 cm length (from tip to shoot) as one replicate were incubated in the reaction mixture for 30 min in the dark at room temperature. The fluorescence intensity was quantified with a fluorescence microplate reader (Infinite® 200 PRO; Tecan, Maennedorf, Switzerland) with an excitation at 540 nm and emission at 610 nm. Different concentrations of H_2O_2 solution were used to prepare the standard curve. The reaction mixture without the substrate or root material served as a control.

Statistical analysis

For all of the pairwise comparisons relative to control groups, Student's *t*-test was performed ($P \leq 0.05$). In the experiments of NAA/IAA complementation with or without smoke addition, linear regression modeling was performed and ANOVA was applied for significance test. For all other experiments, one-way ANOVA was conducted, followed by either Tukey's HSD for symmetric groups or Fisher's protected LSD for unequal groups.

Nucleotide sequence accession numbers

The RNA sequencing data have been deposited in the National Center for Biotechnology Information (NCBI) under project number PRJNA320036.

Results

Smoke cues impair root hair elongation and increase primary root length by regulating cell expansion in the elongation/differentiation zone

In order to determine the potential roles of smoke cues for establishing seedlings, we germinated *Nicotiana attenuata* on media containing different amounts of liquid smoke and observed root morphology. After being treated with liquid smoke, *N. attenuata* primary roots were significantly longer and had more lateral roots, whereas root hair elongation was impaired (Fig. 1). Hypocotyl length did not change. The effect of smoke on root growth and lateral formation was dose-dependent: growth was promoted at low concentrations and inhibited at high concentrations (Figs 1a, S1a,b).

In order to examine whether an increase in cell division in the meristem zone (MZ) or increase in cell expansion in the elongation/differentiation zone (EZ/DZ) accounted for the increase in root length, the number of cortex cells was counted from the quiescent center (QC) to the first elongated cell as a measure of meristem size (Fig. S2a). The number of cells in the MZ did not increase significantly (Fig. 1d); however, the cortical cell length in the EZ/DZ increased significantly (Fig. 1e). Short-term treatments (16 h) with smoke showed the same result as long-term treatments. These results indicate that an increase in longitudinal cell expansion in the EZ/DZ was mainly responsible for the accelerated root growth by smoke cues (Fig. S2).

Catechol, but not karrikins, is the main active compound in smoke that affects root growth

Karrikins were identified in smoke and their effect on seed germination and seedling growth has been well described. However, although treatment with KAR1 dramatically increased the seed germination ratio and decreased hypocotyl elongation, as reported earlier (Flematti *et al.*, 2004a; Nelson *et al.*, 2009), no significant changes in root growth were observed after treatment (Fig. S1c–f).

In order to identify the potential compounds in liquid smoke responsible for the observed increase in primary root elongation and the decrease in root hair growth, bioassay-driven SPE was applied as the first fractionation step. Among the seven collected fractions (S0–S6), only fraction S2 induced the smoke-elicited root phenotype: root length increased and root hair expansion was impaired (Figs 2a, S3). In contrast to the strong acidic smoke solution (1/900, pH 4.2), fraction S2 did not alter the pH of the culture medium, allowing us to rule out the hypothesis that pH changes in the medium are responsible for the root phenotype.

Further fractionation of the active S2 fraction was performed by HPLC. Bioassays were conducted with pooled elutions as indicated in Fig. 2(b). Only treatment with one of the fractions ('d') was able to mimic the root phenotype elicited by S2 (Fig. 2b). Five subfractions (d1–d5) of fraction 'd' were collected, and the application of fraction d3 and d4 resulted in impaired root hair elongation (Fig. 2c).

Based on the acquired masses and retention time, fractions d3 and d4 were identical (Fig. 3a) and pooled for one-dimensional (^{1}H and ^{13}C NMR) and two-dimensional (HSQC) NMR. The ^{1}H NMR spectrum showed two multiplet signals (*ddd*, 3.7/3.7/9.5 Hz) in the aromatic range, at δ_H6.74 and δ_H6.65, respectively, which is typical for a symmetrically 1,2-disubstituted aromatic ring. ^{13}C NMR showed, in accordance with the expectation symmetry, three signals at δ_C116.4, 120.9 and 146.4. Correlations in the ^{1}H-^{13}C HSQC allowed for the final identification of 1,2-dihydroxybenzene (catechol) (Fig. 3b). The

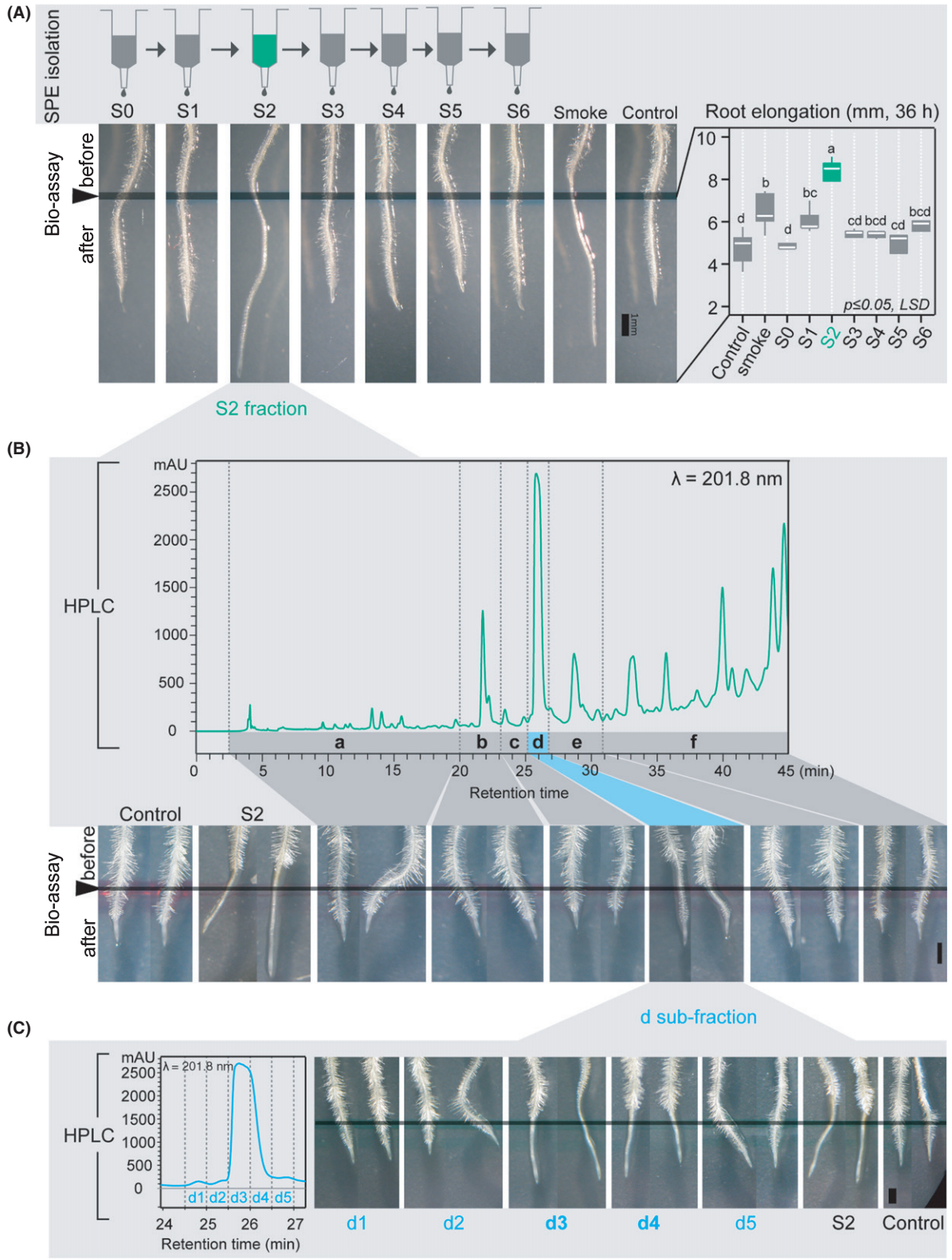

amounts of catechol in liquid smoke (1/900) and active S2 (1/100) were measured by U(H)PLC/ESI-TOF using different catechol concentrations for a standard curve. Both solutions contained approximately half (5.4 μM and 4.9 μM, respectively, Fig. 3c) of the concentration of pure catechol (10 μM) required to elicit a similar extent of root elongation (Fig. 3d). In order to verify whether catechol is the active compound leading to the same root phenotype as that induced by smoke, the bioassay was

Fig. 2 Bioassay-driven solid phase extraction (SPE) and high performance liquid chromatography (HPLC) fractionation: The elution S2 and HPLC fractions d3/d4 are the bioactive fractions in liquid smoke. (A) Scheme of the SPE fractionation procedure and root-phenotype-guided activity assay. Elution S2 is the active fraction of the SPE fractionation. Liquid smoke was loaded onto reverse/cation exchange phase column; the initial flow-through was called S0, and subsequent flow-throughs were referred to as S1–S6. For the bioassay, seedlings were transferred from mock GB5 media to media supplemented with the different elutions (S0–S6). 36 h after transfer, the newly elongated part of the root was measured ($n = 3$, for each biological replicate, 8–12 *Nicotiana attenuata* seedlings per Petri dish were measured); different letters indicate significant differences ($P \leq 0.05$, one-way ANOVA followed by Fisher's LSD). For additional replicates of root hair phenotype, see Supporting Information Fig. S3. The light-colored 'roots' in the pictures are reflections of the roots on the medium due to the photographing technique. (B) HPLC fractionation of SPE-elution S2 on a reversed phase C18 column. Fractions were collected every 30 s; and based on the chromatogram fractions 2.5–20 min, 20–23 min, 23–25 min, 25–27 min, 27–31 min and 31–45 min, fractions were pooled and labeled 'a' through 'f' respectively. Only fraction 'd' inhibited root hair elongation. (C) The further fractionation of fraction 'd', the 5 sub-fractions (d1–d5, starting at 24.5 min) were collected and used for bioassays; both 'd3' and 'd4' decreased root hair elongation. (B, C) Seedlings (5 d post-germination (dpg)) were transferred to media supplemented with the different fraction for 24 h for root hair phenotyping (for each group, 8–10 seedlings per Petri dish were observed). Bars, 1 mm.

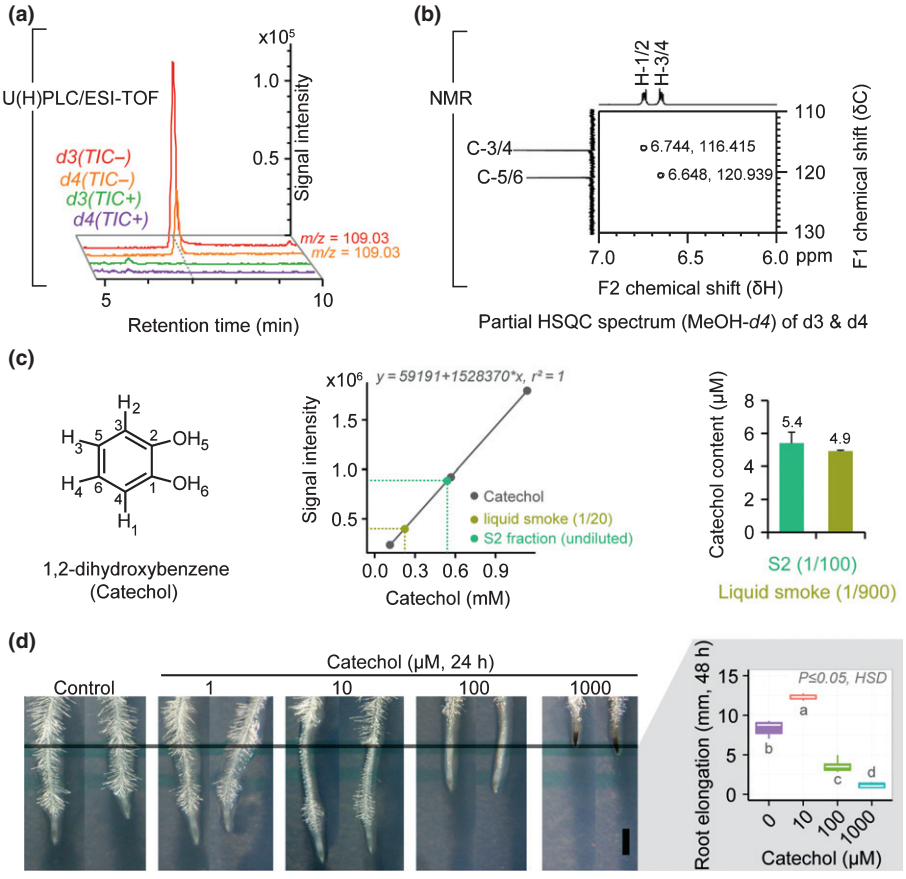

Fig. 3 Mass acquisition by ultra (high) performance liquid chromatography (U(H)PLC)/ electrospray ionization-time of flight (ESI-TOF) and structure elucidation by NMR: catechol is the main active compound in liquid smoke. (a) Mass acquisition by U(H)PLC/ESI-TOF of fractions 'd3' and 'd4' in a negative ionization mode (TIC: total ion chromatogram; –/+: negative/positive ionization mode). (b) Structure elucidation of pooled 'd3' and 'd4' by ^{1}H NMR, ^{13}C NMR and ^{1}H-^{13}C HSQC spectra. (c) NMR revealed that the active compound is catechol. The content of catechol from diluted liquid smoke (1 : 900) and S2 fraction (1 : 100) was quantified by standard curve method. (d) Bioassay with catechol treatment. *Nicotiana attenuata* seedlings (5 d post-germination (dpg)) were transferred to media supplemented with different doses of catechol for 24 h for root hair phenotyping and for 48 h for root elongation measurements. The newly elongated root part after transfer was measured ($n = 6$, for each replicate 25–30 seedlings were measured); different letters indicate significant differences ($P \leq 0.05$, one-way ANOVA followed by Tukey's HSD). Bar, 1 mm (see also Supporting Information Figs S4, S5).

performed using different concentrations of commercially available pure catechol. Both catechol and smoke/S2 showed the same dose-dependent root morphology (Fig. 3d). Interestingly, root elongation was reliably increased up to a concentration of 60 µM, whereas root hair formation was partially impaired by the addition of 10 µM catechol and fully abolished at catechol concentrations higher than 20 µM (Fig. S4).

Several substances whose chemical structures are similar to the structure of catechol but show different levels of redox reactivity, such as resorcinol, hydroquinone and guaiacol, also have been identified in liquid smoke (Baldwin *et al.*, 1994). A comparison of the three isomers of dihydroxybenzene (1,2-dihydroxybenzene-catechol; 1,3-dihydroxybenzene-resorcinol; and 1,4-dihydroxybenzene-hydroquinone) revealed that only catechol impaired root hair elongation and induced root elongation at a concentration of 10 µM, whereas for the para-isomer hydroquinone, a higher concentration was required to observe the effect on root hair growth, and for the meta-isomer resorcinol as well as for guaiacol, a higher concentration was required to induce both, root hair growth and primary root elongation (Fig. S5). Taken together, roots were most sensitive to catechol. We assume that catechol is the main active compound in smoke responsible for inducing the root morphology.

In order to prove that catechol is present not only in liquid smoke, but also under natural conditions, we collected freshly burnt soil from *N. attenuata*'s habitat in Arizona, USA, and *c.* 10.1 µg of catechol in 12.5 g of soil was measured by U(H)PLC/ESI-qTOF (Fig. 4).

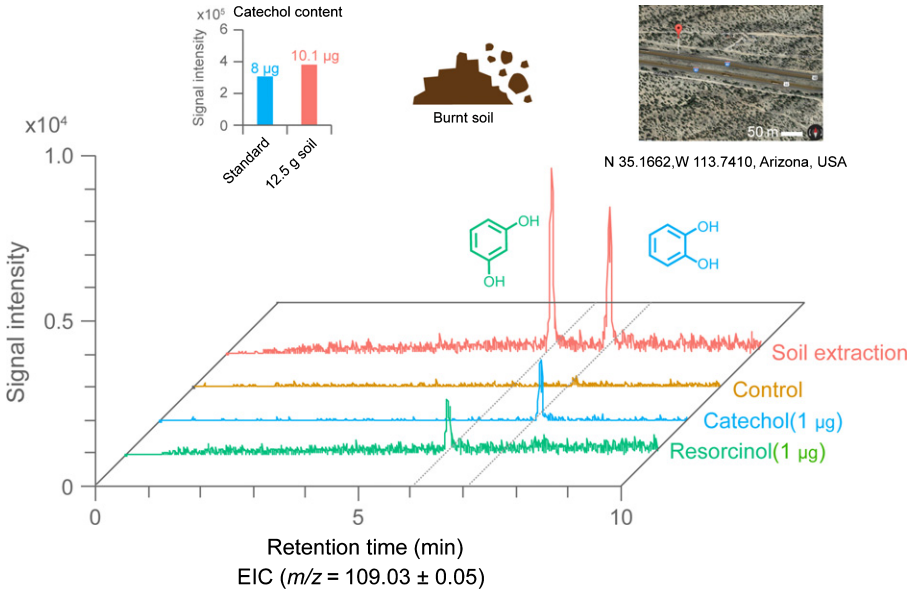

Fig. 4 Catechol occurs in high concentrations (µg g^{-1}) in burnt soil collected from the native habitat of *Nicotiana attenuata*. Catechol and resorcinol were detected by ultra performance liquid chromatography (UPLC)/ electrospray ionization-quadrupole time of flight (ESI-qTOF in extracts from burnt soil. Extracted ion chromatograms (EIC, $m/z = 109.03 \pm 0.05$) of soil extraction (pink) and standards including catechol (cyan) and resorcinol (green). Burnt soil was collected in 2016 from the native habitat of *N. attenuata* in Arizona, USA (inset: Google Map image of collection site).

Smoke-treatment leads to massive changes in gene expression

In order to dissect the potential mechanisms leading to the smoke-induced changes in root morphology, transcriptome profiling was performed by RNA-seq. We used roots treated with the S2 fraction for these analyses, because in contrast to the nonfractionated liquid smoke solution, S2 did not affect the pH of the medium; however, it is more stable than pure catechol, presumably due to the presence of additional compounds in the smoke solution which protect catechol from oxidation. Seedlings were treated with S2-free or S2-containing medium for 2 and 6 h (Fig. 5a). After sequencing, a total of 1391 differentially expressed genes (DEG) were identified ($|\log_2 FC| > 1$, FDR ≤ 0.05; Fig. 5a,b; Table S1).

In order to reveal the main regulatory pathway(s), DEGs at both time points were considered first (424 DEGs; Fig. 5b). Among these, several extensin-like proteins were most strongly downregulated after treatment with smoke (Fig. S6c), whereas a number of glucosyltransferases – *ap2 erf* domain-containing transcription factors and glutathione-S-transferases – were most strongly upregulated (Table S1). A GO analysis of these DEGs showed that enriched networks were mapped mainly to flavonoid biosynthesis, secondary metabolite catabolism, glucosyltransferase, cell redox homeostasis and auxin biosynthesis (Fig. 5c). The two enriched processes – auxin biosynthesis (Zhao, 2010) and cell redox homeostasis (Tsukagoshi, 2016) – are known to play major roles in root development and growth. Networks of enriched GOs for genes differentially expressed only after 2 or 6 h were mainly related to programmed cell death, water transport and general functions such as nucleosome assembly, ribosome and carbohydrate catabolism (Fig. S6a,b).

The smoke-induced root phenotype is not primarily regulated by auxin

We first tested the hypothesis that smoke-induced primary root growth was due to changes in auxin production. Two auxin biosynthesis inhibitors, Kyn and yucasin, were applied and the root phenotypes observed. Kyn is an alternative substrate for L-tryptophan-pyruvate aminotransferase 1 (TAA1) and decreases root-derived auxin production through competition (He *et al.*, 2011). Yucasin is a potent auxin biosynthesis inhibitor that blocks the conversion of indole-3-pyruvic acid (IPyA) to IAA by targeting the YUC enzymes (Nishimura *et al.*, 2014) (Fig. 6a). *Nicotiana attenuata* seedlings grown on medium supplemented with either a range of Kyn concentrations or yucasin, showed increased root length and impaired root hair growth (Fig. 6b,c). By contrast, seedlings grown on NPA-supplemented medium, which is a polar auxin transport inhibitor (Jensen *et al.*, 1998), had an inhibitory effect on root growth (Fig. 6c). At first glance, these results suggested that reduced auxin biosynthesis might be responsible for the smoke-induced phenotype but not for polar auxin transport. However, the quantification of auxin levels in roots after long-term treatment with smoke and short-term treatment with catechol resulted in higher levels of IAA (Fig. 7a) and not the lower levels suggested by the application of the auxin biosynthesis inhibitors. Additionally, we monitored the auxin response in real time by using an auxin reporter line from Arabidopsis (DII-VENUS) which negatively correlates auxin responses with fluorescence intensity. As expected, the application of the auxin biosynthesis inhibitor Kyn resulted in more fluorescence and the application of external auxin resulted in less fluorescence. The addition of smoke and S2 fractions led to an intermediate reduction in fluorescence intensity indicating an increase in auxin levels, as was expected (Fig. S7a,b).

In order to further dissect a possible role for auxin in the smoke-induced root phenotype, we performed a histochemical analysis. The addition of the synthetic auxin NAA (1 nM) led to a significant

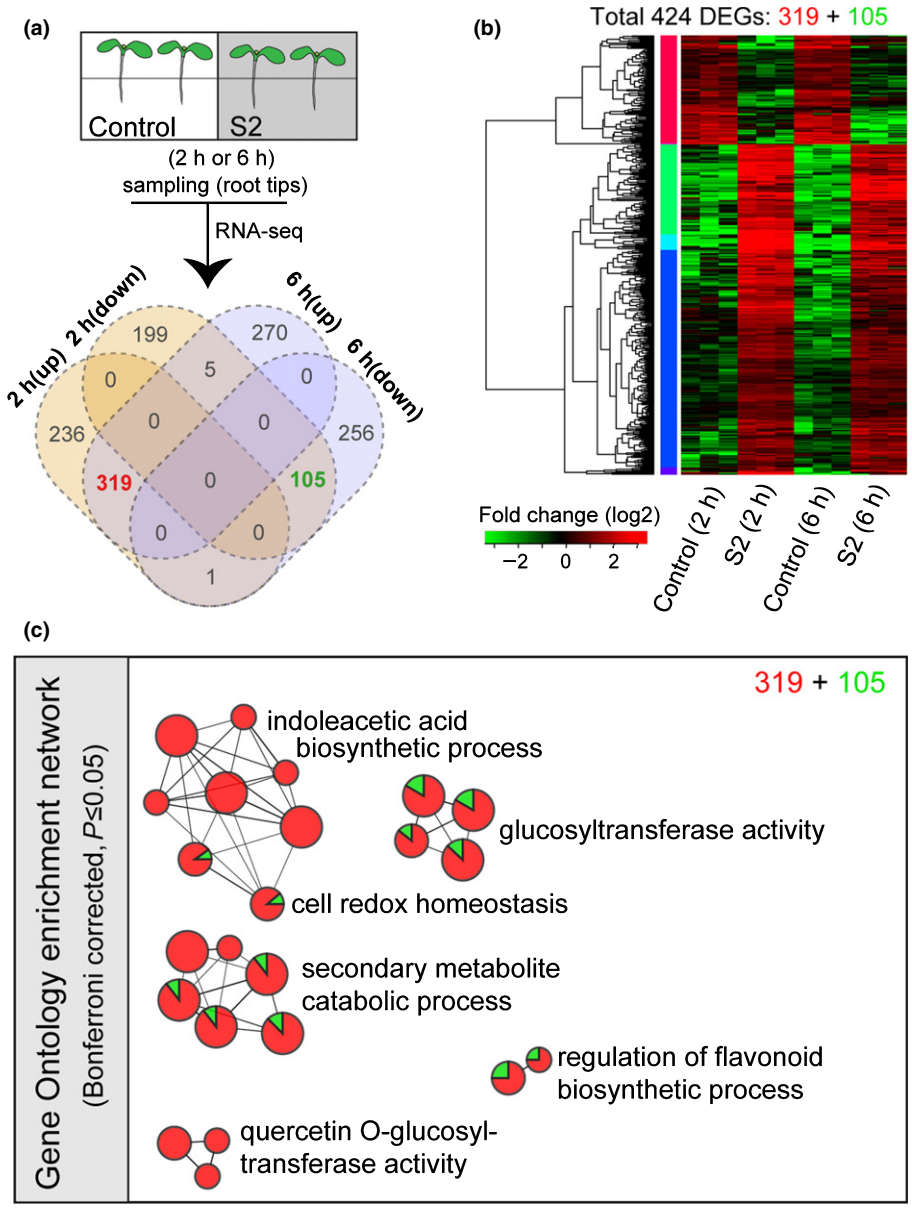

Fig. 5 Hierarchical clustering and the functional enrichment of differentially expressed genes (DEGs) in *Nicotiana attenuata* roots after treatment with the active SPE-elution S2 for 2 and 6 h: genes related to cell redox-homeostasis and auxin biosynthesis are enriched among the upregulated genes at both time-points after treatment. Seedlings (5 d post-germination (dpg)) were transferred to media with or without the S2 fraction, and root tips were harvested for RNA-seq. Three replicates were sequenced for each group (~300 seedlings were harvested from 10 Petri dishes and pooled as one replicate). (a) Sample preparation and data analysis ($|\log_2 FC| > 1$, FDR ≤ 0.05); Venn-diagrams show the number of up- and downregulated genes in root tips after treatment with S2 fraction for 2 and 6 h compared to control groups. Numbers in red (upregulation) and green (downregulation) indicate DEGs (319 + 109) showing the same expression pattern at both time points. (b) Hierarchical cluster analysis of these 424 DEGs. (c) Gene ontology (GO) enrichment analysis of the 424 DEGs was computed with CluGO according to the GO categories 'Biological Process' and 'Molecular Function' (two-sided hypergeometric test, Bonferroni corrected, $P \leq 0.05$) (see also Supporting Information Fig. S6).

increase in the number of MZ cells, whereas the addition of smoke did not significantly alter the number of MZ cells (Fig. 7b). Furthermore, a chemical complementation assay demonstrated that the smoke-induced phenotype could neither be mimicked nor rescued by IAA/NAA treatments (Fig. 7c). Moreover, *SHY2/IAA3*, a key transcription factor involved in controlling the balance of cell division and cell differentiation and considered as a molecular marker of auxin activity, did not respond to S2 fraction incubation based on RNA-seq datasets (Fig. S7c). Taken together, these results indicate that auxin is not the primary signal responsible for the smoke-induced changes in primary root growth and root hair elongation.

Redox processes regulate root growth and root hair elongation in response to smoke

H_2O_2 and O_2^-, two important ROS in roots, are differentially distributed and fulfill different developmental functions. Based on the GO enrichment analysis from the RNA-seq data, we hypothesized that the observed increased cell expansion in the EZ/DZ was due to redox changes. We quantified the content of H_2O_2 and O_2^- in roots before and after catechol exposure, and also exposed roots to salicylhydroxamic acid (SHAM), an inhibitor of peroxidase activity (Brouwer *et al.*, 1986), and DPI, which primarily inhibits NADPH oxidase activity (Li & Trush, 1998). The two inhibitors confirmed the validity of the methodology; their application strongly reduced O_2^- levels. Treating seedlings with different concentrations of catechol also reduced O_2^- production compared to controls (Fig. 8a,b). By contrast, H_2O_2 content did not change in response to catechol treatment (10 μM), but slightly and significantly increased with higher amounts of catechol (Fig. 8c).

In order to understand how catechol treatment affects the levels and distribution of H_2O_2 in the roots, we investigated the spatial distribution of H_2O_2 in response to catechol treatment

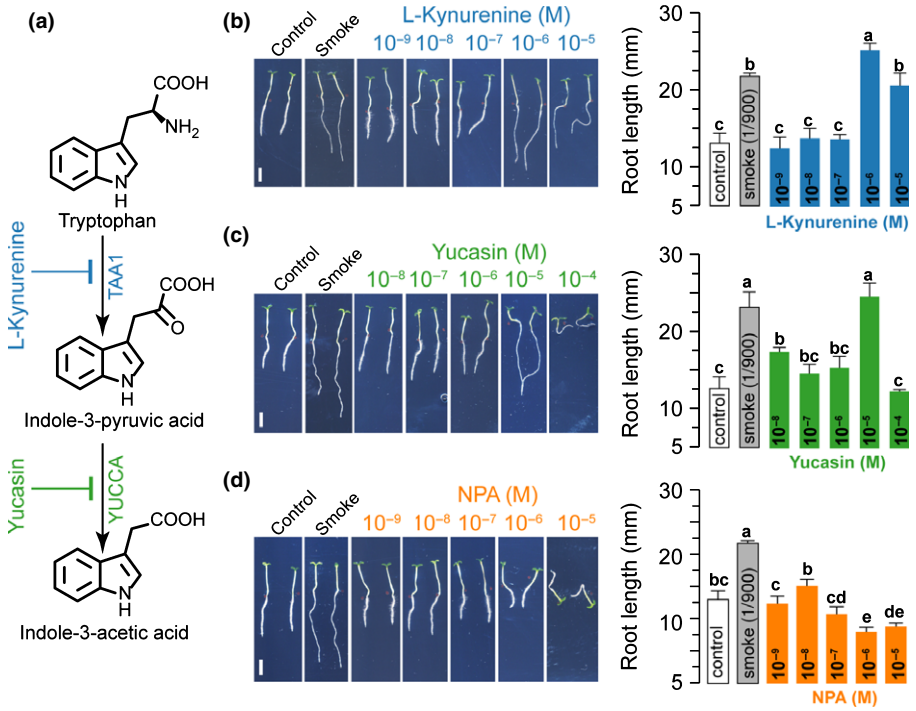

Fig. 6 The root phenotype induced by smoke is mimicked by the application of auxin biosynthesis inhibitors, but not by an auxin transport inhibitor. To investigate if auxin levels are responsible for the smoke-induced root phenotype, auxin biosynthesis and transport inhibitors were applied in an attempt to mimic smoke-induced root phenotype. (a) Auxin biosynthesis is inhibited by L-kynurenine (Kyn) and yucasin. (b, c) Both Kyn and yucasin application mimicked the smoke-induced root phenotype in a concentration-dependent manner. (d) Roots were treated with1-N-naphthylphthalamic acid (NPA), an inhibitor of polar auxin transport. After treatment, root elongation was significantly decreased. (b–d) *Nicotiana attenuata* seedlings were grown on GB5 medium supplemented with different concentrations of Kyn, yucasin and NPA for 9 d (7 d post-germination (dpg)). Data are means + SD ($n = 6$, for each replicate 25–30 seedlings per Petri dish were measured); different letters indicate significant differences ($P \leq 0.05$, one-way ANOVA followed by Tukey's HSD). Bars, 5 mm.

using the highly specific H_2O_2 fluorescent indicator BES-H_2O_2-AC (Maeda, 2008). In controls, H_2O_2 fluorescence was particularly enriched in the expanding root hairs and in the EZ/DZ of primary roots. The strongest signal was found in the cortical cells close to the cell wall, whereas the remaining root parts did not show detectable fluorescence (Fig. 8d). This distribution of ROS is consistent with that found in previous studies (Dunand *et al.*, 2007). However, after catechol treatment, the H_2O_2 fluorescence signal was enriched mainly in the inner tissue surrounding the central cylinder in the EZ/DZ, whereas it disappeared from the outer layers (Fig. 8d). Counterstaining with PI corroborated the observation that after catechol treatment, H_2O_2 was detected in the stele but not around the cortical cell walls, as was observed in the controls (Fig. 6e). We therefore inferred that treating roots with catechol leads to the redistribution of H_2O_2. We speculated that the locally reduced H_2O_2 levels around the cortical cells might be one important factor controlling cell expansion and root hair elongation.

In order to test this hypothesis, we supplemented the catechol-treated roots with H_2O_2. The application of H_2O_2 could partly rescue the catechol-induced phenotype, and a weak H_2O_2 fluorescent signal was detected around the cell walls of the outer layer of cortical cells (Fig. 8e). Furthermore, the additional H_2O_2 supplementation reversed the inhibitory effect of catechol on root hair elongation, and primary root growth rates were similar to those of controls (Fig. 9). However, the phenotype was fully restored only when 100 μM H_2O_2 and 10 μM catechol were applied, whereas higher catechol concentrations and 100 μM H_2O_2 were not able to rescue the root hair development and resulted in significantly reduced root growth (Fig. 9). Based on these results, we conclude that catechol profoundly influences the root morphology by locally decreasing H_2O_2 levels in the cell wall of the cortical layer in the EZ/DZ and thereby increasing H_2O_2 levels in and around the stele.

Discussion

The effects of smoke on seed germination and on the isolation and characterization of active compounds from smoke for enhancing germination have been well documented (Nelson *et al.*, 2012). However, the role of smoke signals on root growth and development is poorly understood. As primary root growth for nutrient uptake is a crucial factor for seedling establishment, it plays a central role in *Nicotiana attenuata*'s ability to colonize the post-fire environment. Here, we identified catechol – which has been shown previously to be highly abundant in smoke (Baldwin *et al.*, 1994; Montazeri *et al.*, 2013) – as the active effector in smoke that morphologically promotes root growth and lateral root formation, while repressing root hair elongation of *N. attenuata* seedlings. We could rule out the germination stimulant karrikin from causing this effect (Figs 1, S1), which indicates

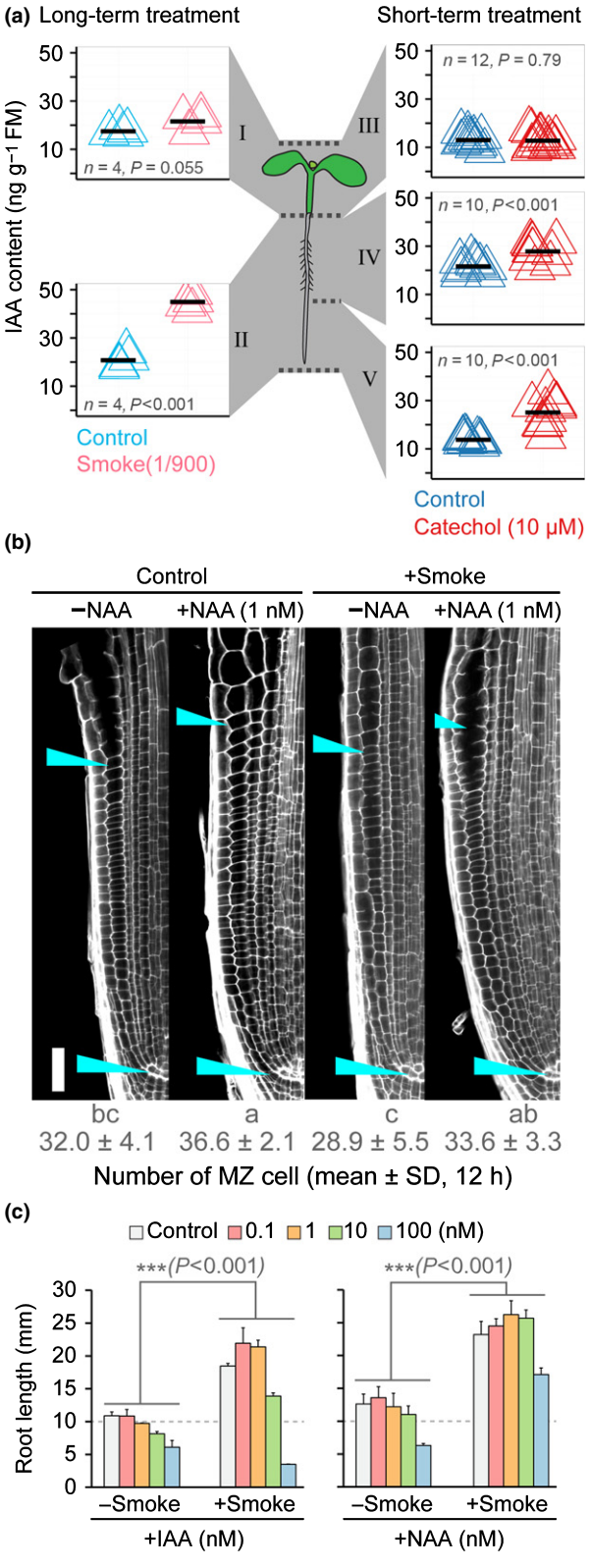

Fig. 7 The smoke-induced root phenotype is not primarily regulated by auxin. (a) Auxin levels were slightly but significantly increased by long-term (left panel) and short-term (right panel) treatment. For long-term treatment, *Nicotiana attenuata* seedlings were grown on media supplemented with liquid smoke for 7 d (5 d post-germination (dpg)); shoot (I) and root (II) were harvested separately. For short-term treatments, seedlings (5 dpg) were treated with catechol (10 µM) for 48 h, and three parts were collected separately (shoot part (III), newly elongated root part after transfer (V) and the remaining part (IV)). Auxin (IAA) was measured by high-resolution LC/MS relative to labeled D-IAA. Cross-bars in the strip plot indicate the means, Student's *t*-test. 420–450 seedlings from 15 Petri dishes were collected as one replicate. (b) The size of the meristem was not significantly altered by smoke induction compared to its size in control groups. Short-term (12 h) application of NAA (1 nM) increased the number of meristem zone (MZ) cells, but results from treatment with external smoke plus supplementation with NAA did not significantly differ from results from the application of NAA only. The distances of MZ (left half only) for measuring are marked by arrow-heads. Data are means ± SD (15–20 seedlings were analyzed, only the left half of root was counted), different letters indicate significances ($P \leq 0.05$, one-way ANOVA followed by Fisher's LSD). (c) Chemical complementation assay. Indole-acetic acid (IAA) and the synthetic auxin, 1-naphthaleneacetic acid (NAA) did not rescue the faster primary root elongation induced by smoke (v/v = 1/900) application. Seedlings were grown on GB5 media with external supplementations as indicated (7 dpg). Data are means ± SD ($n = 6$, for each replicate 25–30 seedlings per Petri dish were measured; linear regression model was applied followed by ANOVA test: ***, $P \leq 0.001$) (see also Supporting Information Fig. S7).

that *N. attenuata* perceives different substances in smoke responsible for germinating and establishing seedlings.

The transcriptome profiling and gene ontology (GO) network analysis indicated that auxin biosynthesis and redox-homeostasis were affected by smoke cues. Previous studies characterizing the morphology of the roots of Arabidopsis auxin biosynthesis mutants (Pitts *et al.*, 1998) and of roots exposed to an imbalance of H_2O_2 and O_2^- (Takeda *et al.*, 2008) describe similar phenotypes. Based on the similarities of the observed root phenotype after treatment with smoke and the auxin-biosynthesis inhibitors Kyn and yucasin (Nishimura *et al.*, 2014), we initially assumed that the inhibition of auxin biosynthesis and, hence, decreased auxin levels, might be an important factor in tobacco's response to smoke. However, our results strongly suggest that auxin biosynthesis does not play a primary role in the smoke- and catechol-induced root phenotype because (1) supplementing the smoke-treated roots with auxins could not rescue the phenotype, (2) the total amounts of auxin showed the opposite pattern – they increased in smoke/catechol-treated roots, and (3) the expression of the molecular marker Na*SHY2* regulated by auxin did not significantly change after treatment. Additionally, in agreement with previous publications (Peng *et al.*, 2013; Perrot-Rechenmann, 2013), the treatment of roots with the synthetic auxin NAA increased the number of cells in the meristem zone, whereas the application of smoke did not. Further evidence against a central role of auxin in the smoke-induced phenotype was provided by the Arabidopsis DII-VENUS line, which confirmed a slight increase in auxin levels after smoke treatment; however, this increase in auxin levels was not accompanied by an increased number of MZ cells (Figs 6, 7, S7). It may be that the increase of IAA is a byproduct or secondary signal from the plants' primary physiological responses to smoke treatment. However, an effect of the increased auxin levels on meristem

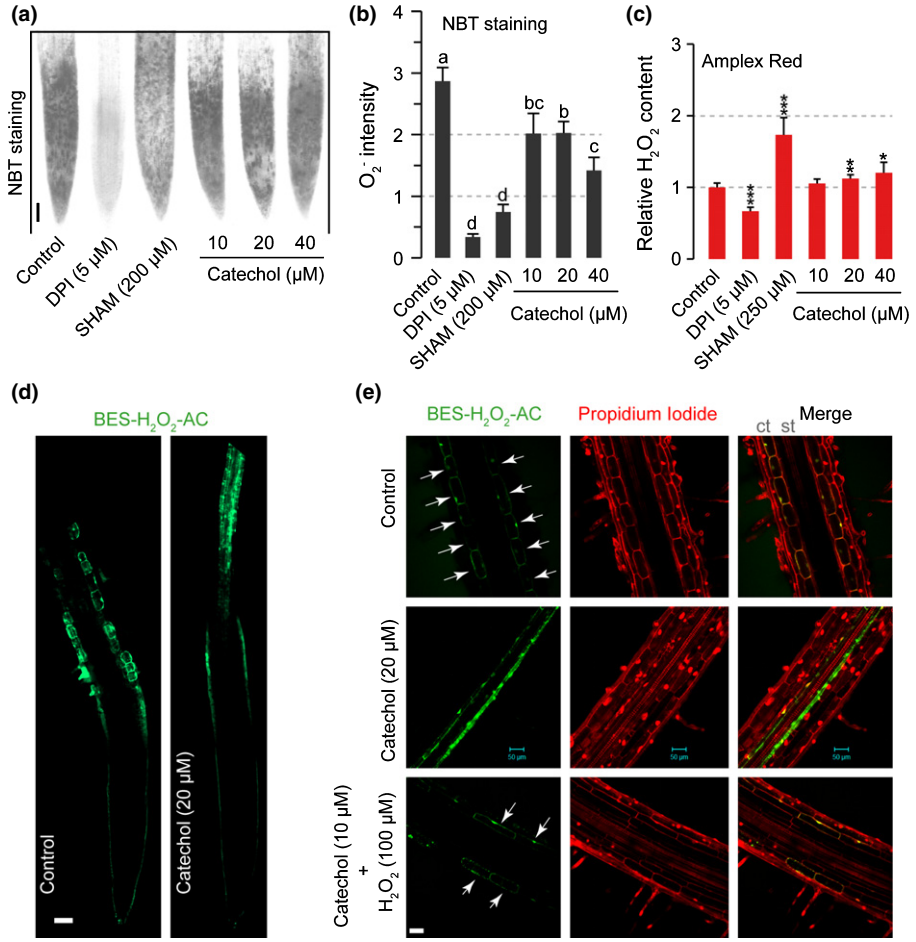

Fig. 8 Localization and total amounts of hydrogen peroxide (H_2O_2) in *Nicotiana attenuata* roots are altered by catechol treatment. (a) Histochemical localization of superoxide anions (O_2^-) by nitroblue tetrazolium (NBT) staining. Seedlings (5 d post-germination (dpg)) were transferred to media containing different concentrations of catechol, diphenyleneiodonium (DPI, NADPH oxidase inhibitor), and salicylhydroxamic acid (SHAM, peroxidase inhibitor), and pictures were taken 12 h after transfer. Bar, 100 µm. (b) O_2^- amounts in roots significantly decreased after catechol incubation by quantification of NBT-stained signals in (a) (data are means + SD, 15–20 seedlings were measured). Different letters indicate significant differences ($P \leq 0.05$, one-way ANOVA followed by Fisher's LSD). (c) Total amounts of H_2O_2 slightly but significantly increased as the concentration of catechol increased in the treatment by Amplex red staining 24 h after induction (means + SD, $n = 4$, for each replicate, 6 newly elongated root parts after transfer were pooled as one replicate). Significant differences relative to the control group are indicated by asterisks (Student's *t*-test: **, $P \leq 0.01$; ***, $P \leq 0.001$). (d) Imaging after BES-H_2O_2-AC staining with LSM 510 microscope (ZEISS) to visualize H_2O_2 spatial distribution in root tip. Bar, 100 µm. (e) Counterstaining BES-H_2O_2-AC with propidium iodide (PI) showed that without treatment, H_2O_2 was enriched around the cortical cells, whereas after catechol treatment, H_2O_2 was mainly enriched in the area around the stele. Seedlings were transferred to media supplemented with catechol and H_2O_2 for 24 h before staining. Arrows indicate H_2O_2 localization around cortical cells (6–10 roots were analyzed). st, stele; ct, cortex. Bars, 50 µm.

zone (MZ) cell proliferation might have been countered by decreased O_2^- levels.

In addition to changes in biosynthesis, signaling and the temporal and spatial distribution of auxin are also crucial to fully evaluate the effects of auxin on growth (Ljung, 2013); in particular, the cell-to-cell transport of auxin can generate auxin gradients that elicit growth responses (Sauer *et al.*, 2013). However, in the present study, the inhibition of auxin transport was unable to mimic the smoke-induced phenotype, which supports the inference that auxin is not the primary effector. Nevertheless, based on the data provided here, highly local cell-to-cell changes in auxin concentrations cannot be ruled out completely.

The observed induction of reactive oxygen species (ROS)-related genes corresponds with the analysis of the transcriptome of maize embryos treated with liquid smoke solution for 24 h; this analysis also demonstrated a GO enrichment for redox processes (Soós *et al.*, 2009). ROS are well-known from the signal transduction pathways that regulate plant growth, development and defense responses (Considine *et al.*, 2015), and their production is tightly controlled and locally restricted (Schmidt & Schippers, 2015). As was shown in histochemical studies in several other plant species (Schopfer, 1994; Dunand *et al.*, 2007; Tsukagoshi *et al.*, 2010), in *N. attenuata* O_2^- was present mainly in inner tissues of the young elongation zone, and, to a lesser extent, in the meristem zone and in the stele along the roots (Fig. 8a). By contrast, H_2O_2 was highly abundant around cell walls of the cortical layer in the elongation/differentiation zone (EZ/DZ) confined to the apoplast and in the expanding root

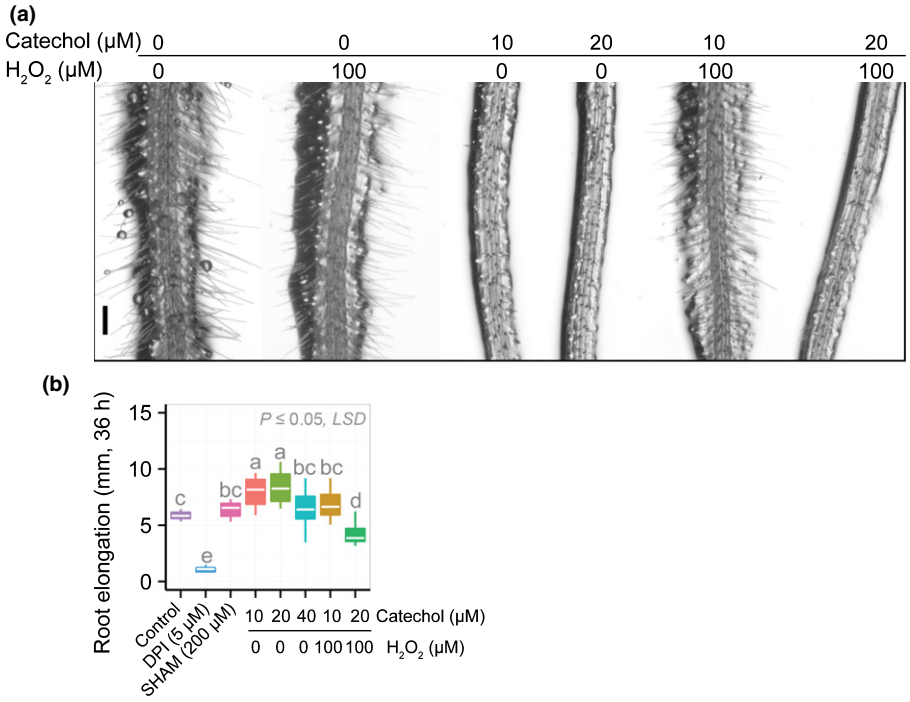

Fig. 9 Hydrogen peroxide (H_2O_2) partially rescues the smoke-induced root phenotype in a defined concentration range. (a) The addition of H_2O_2 restored root hair elongation after catechol treatment. *Nicotiana attentuata* seedlings (5 d post-germination (dpg)) were transferred to media containing catechol and H_2O_2 in different concentrations as indicated. (b) Root lengths from the same set-up as in (a) were partially restored to levels of control. Measurements were taken 36 h after treatment. 20–25 seedlings were analyzed for each treatment, $P \leq 0.05$, one-way ANOVA followed by Fisher's LSD. Box plots show the medium (white horizontal line), the upper and lower quartile (upper and lower end of the box) and the minimum and maximum (whiskers). Bar, 0.25 mm.

hairs (Fig. 8d,e). After treatment with smoke or catechol, only a very weak H_2O_2 signal was detected in this area, whereas a strong H_2O_2 signal appeared in the tissue surrounding the stele. Using compounds with a similar structure but altered antioxidant capacity, we obtained data that were consistent with the idea that changes in the redox homeostasis in the cortex are responsible for enhanced primary root growth and impaired root hair extension: roots were most sensitive to compounds containing free hydroxyl groups and also to the ortho-position of the OH-groups of catechol (Fig. S5). Catechol possesses the highest antioxidant capacity among the three di-hydroxybenzene isomers (Bendary *et al.*, 2013), and it facilitates the Fenton reaction and can be absorbed by membranes (Schweigert *et al.*, 2001).

Different mechanisms may be responsible for root elongation and impaired root hair growth because root elongation occurred at a lower catechol concentration than did root hair growth inhibition (Fig. S4). It is well known that root hair growth in Arabidopsis is strongly decreased after antioxidant treatment (Foreman *et al.*, 2003; Carol & Dolan, 2006); and mutants (*pft1*) impaired in the redox-homeostasis showed impaired root hair differentiation and elongation, and longer roots (Sundaravelpandian *et al.*, 2013). Similarly, here the antioxidant function of catechol may inhibit root hair elongation by locally disturbing the redox homeostasis, in particular at the root hair tip.

Root growth was not due to an increase in cell numbers, but catechol/smoke-treatment resulted in cell expansion in the EZ/DZ (Fig. 1). This expansion requires the loosening of the cell wall matrix (Wolf *et al.*, 2012). It is possible that the disappearance of H_2O_2 in the cortex of the elongation/differentiation zone is due to catechol's ability to generate hydroxyl radicals (OHs) via the H_2O_2-dependent chelator-driven Fenton reaction (Schweigert *et al.*, 2001). $^{\cdot}$OHs are known to cause polymer cleavage and wall loosening, specifically in the growing zone (Tenhaken, 2014; Kärkönen & Kuchitsu, 2015). The cell wall provides the necessary conditions for this reaction (Schopfer, 2001; Liszkay *et al.*, 2004; Kim *et al.*, 2014) due to the presence of iron ions and peroxidases class III, all of which have H_2O_2-producing and scavenging abilities that depend on the chemical environment (Price *et al.*, 2003; Passardi *et al.*, 2004b).

Interestingly, although the H_2O_2 signal disappeared in the apoplast, a fluorescent signal indicating the presence of H_2O_2 appeared around the stele; however, total amounts of H_2O_2 in the roots were not altered (Fig. 8). We propose that either catechol or ROS themselves cross the plasma membrane (Schweigert *et al.*, 2001) and react in the cell, or that a catechol-induced redox signal is transduced from the cell wall into the cell. In this context it is important to note that the transcriptome data revealed changes in both the transcriptional expression of genes related to the highly regulated enzymes involved in ROS formation including glutathione peroxidase (GPX), catalase (CAT), superoxide dismutase (SOD), respiratory burst oxidase homolog D (RBOHD) and peroxidases after treatment with smoke fraction S2, and also in many transcription factors, extensins (EXTs) and receptor-like kinases (RLK) (Table S1).

The strong downregulation of EXT-like proteins shows an interesting parallel with mutants impaired in EXT expression (Fig. S6c), such as the leucine-rich repeat extensins 1 and 2 (*lrx1* and *lrx2*) with aberrant root hair formation (Ringli, 2010) and T-DNA homozygous mutant lines (*ext6, ext7, ext10*) with strongly reduced root hairs (Velasquez *et al.*, 2011). EXTs are known to be hydroxylated, and subsequently O-glycosylated and cross-linked with other EXTs to form a network in the plant cell wall. This cross-linking process requires EXT-specific peroxidases of type III and ROS (Passardi *et al.*, 2004a; Velasquez *et al.*,

2011). Considering the gene expression changes in ROS-related genes and the strong downregulation of EXTs upon elicitation with smoke cues, we propose that catechol/smoke treatment weakens the cross-linking in the cell wall we propose that catechol/smoke treatment weakens the cross-linking in the cell wall and that this weakening is due to the lack of structural extensins. However, to confirm this hypothesis, the signal leading to reduced EXT expression still has to be elucidated.

Recent results indicate that five members of an RLK subfamily in Arabidopsis are cell wall sensors; homologs of two (*RLK-theseus 1* and *-feronia*) (Cheung & Wu, 2011; Lindner *et al.*, 2012) are also regulated after smoke treatment (Table S1). RLK-feronia has been thought to activate the production of ROS, and these regulate growth (Cheung & Wu, 2011). It is tempting to speculate that ROS perceive local changes in the redox-state in the apoplast in the presence of smoke-inducing signaling cascades, and that these changes ultimately result in growth effects.

catechol at high concentrations has been well described as a highly toxic organic industrial waste product (Petriccione *et al.*, 2013), yet its role in root growth for fire ephemerals has not been studied previously. In the present study we show that catechol is not only present in liquid smoke solution, but also occurs at high concentrations ($\mu g\, g^{-1}$) in freshly burned soil from the wild tobacco plant's native habitat (Fig. 4). Plant roots forage in the soil for minerals and water (Trewavas, 2014). We assume that the root phenotype observed *in vitro* is of ecological importance. The catechol-induced root elongation and increase in the number of lateral roots may enable the roots to grow more quickly into areas of the highest nutrient concentrations. However, additional research is needed to better understand the local distribution and persistence of catechol in burned soil and its correlation with the presence of nutrients, and to fully understand its ecological role as an environmental signal.

In conclusion, we provide evidence that, depending on the dose, smoke can induce root growth and suppress root hair elongation in *N. attenuata* seedlings. Smoke-induced root development changes were mainly mediated by catechol. Transcriptomic sequencing suggests that although the expression of genes from both auxin biosynthesis and ROS pathways was significantly altered by smoke treatment, only ROS were found to be involved directly in smoke-induced root development changes and these acted by altering the distribution of H_2O_2 in the elongation zone. Further experiments will be required to elucidate how the catechol-induced changes in the redox state are sensed in the root, if catechol is also transported into the cells, and whether the presence of catechol in the soil will promote plant growth and fitness in the field.

Acknowledgements

We thank Nam Nguyen, Zach Liechty and Irem Tuyusz for help with seedling growth and harvest; Klaus Gase for assistance with RNA-seq data submission, Jürgen Rybak for LSM instructions and Emily Wheeler for editorial assistance. This study was funded by the Max Planck Society, by Advanced Grant 293926 from the European Research Council to ITB, and by the Collaborative Research Centre 'Chemical Mediators in Complex Biosystems – ChemBioSys' (SFB 1127). S.X. acknowledges funding by the SNF (PEBZP3-142886) and a Marie Curie Intra-European-Fellowship (328935).

Author contributions

M.W., I.T.B. and K.G. planned and designed the research and wrote the manuscript; M.W. performed the research and analyzed the data; M.S. guided the fractionation of catechol and its analysis by HPLC and MS; S.X. annotated the RNA-seq data and helped with RNA-seq data analysis; C.P. undertook the NMR analysis; and J.W. contributed to data collection.

References

Abdelgadir H, Kulkarni M, Arruda M, Van Staden J. 2012. Enhancing seedling growth of *Jatropha curcas*—a potential oil seed crop for biodiesel. *South African Journal of Botany* **78**: 88–95.

Abdollahi M. 2012. Effect of plant-derived smoke on germination, seedling vigour and growth of rapeseed (*Brassica napus*) under laboratory and greenhouse conditions. *Seed Science and Technology* **40**: 437–442.

Adamowski M, Friml J. 2015. PIN-dependent auxin transport: action, regulation, and evolution. *Plant Cell* **27**: 20–32.

Anders S, Pyl PT, Huber W. 2014. HTSeq – a Python framework to work with high-throughput sequencing data. *Bioinformatics* **31**: 166–169.

Baldwin IT, Morse L. 1994. Up in smoke 2. Germination of *Nicotiana attenuata* in response to smoke-derived cues and nutrients in burned and unburned soils. *Journal of Chemical Ecology* **20**: 2373–2391.

Baldwin IT, Staszakkozinski L, Davidson R. 1994. Up in smoke 1. Smoke-derived germination cues for postfire annual, *Nicotiana attenuata* Torr ex Watson. *Journal of Chemical Ecology* **20**: 2345–2371.

Bendary E, Francis R, Ali H, Sarwat M, El Hady S. 2013. Antioxidant and structure–activity relationships (SARs) of some phenolic and anilines compounds. *Annals of Agricultural Sciences* **58**: 173–181.

Brouwer KS, van Valen T, Day DA, Lambers H. 1986. Hydroxamate-stimulated O_2 uptake in roots of *Pisum sativum* and *Zea mays,* mediated by a peroxidase its consequences for respiration measurements. *Plant Physiology* **82**: 236–240.

Carol RJ, Dolan L. 2006. The role of reactive oxygen species in cell growth: lessons from root hairs. *Journal of Experimental Botany* **57**: 1829–1834.

Cheung AY, Wu H-M. 2011. THESEUS 1, FERONIA and relatives: a family of cell wall-sensing receptor kinases? *Current Opinion in Plant Biology* **14**: 632–641.

Chumpookam J, Lin H-L, Shiesh C-C. 2012. Effect of smoke-water on seed germination and seedling growth of papaya (*Carica papaya* cv. Tainung No. 2). *Horticultural Science* **47**: 741–744.

Considine MJ, Maria Sandalio L, Foyer CH. 2015. Unravelling how plants benefit from ROS and NO reactions, while resisting oxidative stress PREFACE. *Annals of Botany* **116**: 469–473.

Dinneny JR, Benfey PN. 2008. Plant stem cell niches: standing the test of time. *Cell* **132**: 553–557.

Draelants D, Avitabile D, Vanroose W. 2015. Localized auxin peaks in concentration-based transport models of the shoot apical meristem. *Journal of The Royal Society Interface* **12**: 20141407.

Dunand C, Crèvecoeur M, Penel C. 2007. Distribution of superoxide and hydrogen peroxide in Arabidopsis root and their influence on root development: possible interaction with peroxidases. *New Phytologist* **174**: 332–341.

Flematti GR, Ghisalberti EL, Dixon KW, Trengove RD. 2004a. A compound from smoke that promotes seed germination. *Science* **305**: 977.

Flematti GR, Ghisalberti EL, Dixon KW, Trengove RD. 2004b. Molecular weight of a germination-enhancing compound in smoke. *Plant and Soil* **263**: 1–4.

Foreman J, Demidchik V, Bothwell JH, Mylona P, Miedema H, Torres MA, Linstead P, Costa S, Brownlee C, Jones JD. 2003. Reactive oxygen species produced by NADPH oxidase regulate plant cell growth. *Nature* **422**: 442–446.

Foyer CH, Noctor G. 2013. Redox signaling in plants. *Antioxidants and Redox Signaling* **18**: 2087–2090.

Fry SC, Dumville JC, Miller JG. 2001. Fingerprinting of polysaccharides attacked by hydroxyl radicals *in vitro* and in the cell walls of ripening pear fruit. *Biochemical Journal* **357**: 729–737.

Galinha C, Hofhuis H, Luijten M, Willemsen V, Blilou I, Scheres RHB. 2007. PLETHORA proteins as dose-dependent master regulators of Arabidopsis root development. *Nature* **449**: 1053–1057.

Gapper C, Dolan L. 2006. Control of plant development by reactive oxygen species. *Plant Physiology* **141**: 341–345.

Goodspeed TH. 1955. *The genus Nicotiana*. Waltham, MA, USA: Chronica Botanica Company.

Grman E, Robinson TMP. 2013. Resource availability and imbalance affect plant–mycorrhizal interactions: a field test of three hypotheses. *Ecology* **94**: 62–71.

Haas BJ, Papanicolaou A, Yassour M, Grabherr M, Blood PD, Bowden J, Couger MB, Eccles D, Li B, Lieber M *et al.* 2013. De novo transcript sequence reconstruction from RNA-Seq: reference generation and analysis with Trinity. *Nature Protocols* **8**: 1494–1512.

He W, Brumos J, Li H, Ji Y, Ke M, Gong X, Zeng Q, Li W, Zhang X, An F. 2011. A small-molecule screen identifies L-kynurenine as a competitive inhibitor of TAA1/TAR activity in ethylene-directed auxin biosynthesis and root growth in Arabidopsis. *The Plant Cell* **23**: 3944–3960.

Jensen PJ, Hangarter RP, Estelle M. 1998. Auxin transport is required for hypocotyl elongation in light-grown but not dark-grown Arabidopsis. *Plant Physiology* **116**: 455–462.

Kärkönen A, Kuchitsu K. 2015. Reactive oxygen species in cell wall metabolism and development in plants. *Phytochemistry* **112**: 22–32.

Keeley SC, Pizzorno M. 1986. Charred wood stimulated germination of two fire-following herbs of the California chaparral and the role of hemicellulose. *American Journal of Botany* **73**: 1289–1297.

Kim JH, Lee Y, Kim EJ, Gu S, Sohn EJ, Seo YS, An HJ, Chang YS. 2014. Exposure of iron nanoparticles to *Arabidopsis thaliana* enhances root elongation by triggering cell wall loosening. *Environmental Science & Technology* **48**: 3477–3485.

Kim D, Pertea G, Trapnell C, Pimentel H, Kelley R, Salzberg SL. 2013. TopHat2: accurate alignment of transcriptomes in the presence of insertions, deletions and gene fusions. *Genome Biology* **14**: 1–13.

Kruegel T, Lim M, Gase K, Halitschke R, Baldwin IT. 2002. *Agrobacterium*-mediated transformation of *Nicotiana attenuata*, a model ecological expression system. *Chemoecology* **12**: 177–183.

Kulkarni M, Sparg S, Light M, Van Staden J. 2006. Stimulation of rice (*Oryza sativa* L.) seedling vigour by smoke-water and butenolide. *Journal of Agronomy and Crop Science* **192**: 395–398.

Li Y, Trush MA. 1998. Diphenyleneiodonium, an NAD (P) H oxidase inhibitor, also potently inhibits mitochondrial reactive oxygen species production. *Biochemical and Biophysical Research Communications* **253**: 295–299.

Lindgreen S. 2012. AdapterRemoval: easy cleaning of next-generation sequencing reads. *BMC Research Notes* **5**: 1–7.

Lindner H, Mueller LM, Boisson-Dernier A, Grossniklaus U. 2012. CrRLK1L receptor-like kinases: not just another brick in the wall. *Current Opinion in Plant Biology* **15**: 659–669.

Ling Z, Zhou W, Baldwin IT, Xu S. 2015. Insect herbivory elicits genome-wide alternative splicing responses in *Nicotiana attenuata*. *Plant Journal* **84**: 228–243.

Liszkay A, van der Zalm E, Schopfer P. 2004. Production of reactive oxygen intermediates ($O_2^{\cdot-}$, H_2O_2, and OH) by maize roots and their role in wall loosening and elongation growth. *Plant Physiology* **136**: 3114–3123.

Ljung K. 2013. Auxin metabolism and homeostasis during plant development. *Development* **140**: 943–950.

Maeda H. 2008. Which are you watching, an individual reactive oxygen species or total oxidative stress? *Annals of the New York Academy of Sciences* **1130**: 149–156.

Montazeri N, Oliveira AC, Himelbloom BH, Leigh MB, Crapo CA. 2013. Chemical characterization of commercial liquid smoke products. *Food Science and Nutrition* **1**: 102–115.

Nelson DC, Flematti GR, Ghisalberti EL, Dixon KW, Smith SM. 2012. Regulation of seed germination and seedling growth by chemical signals from burning vegetation. *Plant Biology* **63**: 107–130.

Nelson DC, Riseborough JA, Flematti GR, Stevens J, Ghisalberti EL, Dixon KW, Smith SM. 2009. Karrikins discovered in smoke trigger Arabidopsis seed germination by a mechanism requiring gibberellic acid synthesis and light. *Plant Physiology* **149**: 863–873.

Nguema-Ona E, Vicre-Gibouin M, Gotte M, Plancot B, Lerouge P, Bardor M, Driouich A. 2014. Cell wall O-glycoproteins and N-glycoproteins: aspects of biosynthesis and function. *Frontiers in Plant Science* **5**: 12.

Nishimura T, Ki Hayashi, Suzuki H, Gyohda A, Takaoka C, Sakaguchi Y, Matsumoto S, Kasahara H, Sakai T, Ji Kato. 2014. Yucasin is a potent inhibitor of YUCCA, a key enzyme in auxin biosynthesis. *Plant Journal* **77**: 352–366.

Passardi F, Longet D, Penel C, Dunand C. 2004a. The class III peroxidase multigenic in land plants family in rice and its evolution. *Phytochemistry* **65**: 1879–1893.

Passardi F, Penel C, Dunand C. 2004b. Performing the paradoxical: how plant peroxidases modify the cell wall. *Trends in Plant Science* **9**: 534–540.

Peng Q, Wang H, Tong J, Kabir MH, Huang Z, Xiao L. 2013. Effects of indole-3-acetic acid and auxin transport inhibitor on auxin distribution and development of peanut at pegging stage. *Scientia Horticulturae* **162**: 76–81.

Perrot-Rechenmann C. 2013. *Auxin signaling in primary roots*. Boca Raton, FL, USA: CRC Press.

Petriccione M, Forte V, Valente D, Ciniglia C. 2013. DNA integrity of onion root cells under catechol influence. *Environmental Science and Pollution Research* **20**: 4859–4871.

Petricka JJ, Winter CM, Benfey PN. 2012. Control of Arabidopsis root development. *Annual Review of Plant Biology* **63**: 563.

Petrov VD, Van Breusegem F. 2012. Hydrogen peroxide – a central hub for information flow in plant cells. *AoB Plants* **2012**: pls014.

Pitts RJ, Cernac A, Estelle M. 1998. Auxin and ethylene promote root hair elongation in Arabidopsis. *Plant Journal* **16**: 553–560.

Preston CA, Baldwin IT. 1999. Positive and negative signals regulate germination in the post-fire annual, *Nicotiana attenuata*. *Ecology* **80**: 481–494.

Price NJ, Pinheiro C, Soares CM, Ashford DA, Ricardo CP, Jackson PA. 2003. A biochemical and molecular characterization of LEP1, an extensin peroxidase from lupin. *Journal of Biological Chemistry* **278**: 41389–41399.

Rahman A, Bannigan A, Sulaman W, Pechter P, Blancaflor EB, Baskin TI. 2007. Auxin, actin and growth of the *Arabidopsis thaliana* primary root. *Plant Journal* **50**: 514–528.

Raya-González J, Ortiz-Castro R, Ruíz-Herrera LF, Kazan K, López-Bucio J. 2014. PHYTOCHROME AND FLOWERING TIME1/MEDIATOR25 regulates lateral root formation via auxin signaling in Arabidopsis. *Plant Physiology* **165**: 880–894.

Ringli C. 2010. The hydroxyproline-rich glycoprotein domain of the Arabidopsis LRX1 requires Tyr for function but not for insolubilization in the cell wall. *Plant Journal* **63**: 662–669.

Rodríguez-Sanz H, Solís M-T, López M-F, Gómez-Cadenas A, Risueño MC, Testillano PS. 2015. Auxin biosynthesis, accumulation, action and transport are involved in stress-induced microspore embryogenesis initiation and progression in *Brassica napus*. *Plant and Cell Physiology* **56**: 1401–1417.

Rundel P. 1981. Fire as an ecological factor. In: Lange OL, Nobel BS, Osmond CB, Ziegler H, eds. *Physiological plant ecology, vol. 12.* A of the series Encyclopedia of Plant Physiology. Berlin: Springer, 501–538.

Sabatini S, Beis D, Wolkenfelt H, Murfett J, Guilfoyle T, Malamy J, Benfey P, Leyser O, Bechtold N, Weisbeek P *et al.* 1999. An auxin-dependent distal organizer of pattern and polarity in the Arabidopsis root. *Cell* **99**: 463–472.

Sauer M, Robert S, Kleine-Vehn J. 2013. Auxin: simply complicated. *Journal of Experimental Botany* **64**: 2565–2577.

Schaefer M, Brutting C, Baldwin IT, Kallenbach M. 2016. High-throughput quantification of more than 100 primary- and secondary-metabolites, and

phytohormones by a single solid-phase extraction based sample preparation with analysis by UHPLC-HESI-MS/MS. *Plant Methods* **12**: 30.

Schmidt R, Schippers JH. 2015. ROS-mediated redox signaling during cell differentiation in plants. *Biochimica et Biophysica Acta* **1850**: 1497–1508.

Schopfer P. 1994. Histochemical demonstration and localization of H_2O_2 in organs of higher plants by tissue printing on nitrocellulose paper. *Plant Physiology* **104**: 1269–1275.

Schopfer P. 2001. Hydroxyl radical-induced cell-wall loosening in vitro and *in vivo*: implications for the control of elongation growth. *Plant Journal* **28**: 679–688.

Schweigert N, Zehnder AJB, Eggen RIL. 2001. Chemical properties of catechols and their molecular modes of toxic action in cells, from microorganisms to mammals. *Environmental Microbiology* **3**: 81–91.

Soós V, Sebestyén E, Juhász A, Pintér J, Light ME, Van Staden J, Balázs E. 2009. Stress-related genes define essential steps in the response of maize seedlings to smoke-water. *Functional and Integrative Genomics* **9**: 231–242.

Sundaravelpandian K, Chandrika NNP, Schmidt W. 2013. PFT1, a transcriptional mediator complex subunit, controls root hair differentiation through reactive oxygen species (ROS) distribution in Arabidopsis. *New Phytologist* **197**: 151–161.

Takeda S, Gapper C, Kaya H, Bell E, Kuchitsu K, Dolan L. 2008. Local positive feedback regulation determines cell shape in root hair cells. *Science* **319**: 1241–1244.

Taylor J, Van Staden J. 1998. Plant-derived smoke solutions stimulate the growth of *Lycopersicon esculentum* roots in vitro. *Plant Growth Regulation* **26**: 77–83.

Tenhaken R. 2014. Cell wall remodeling under abiotic stress. *Frontiers in Plant Science* **5**: 771.

Tian Q, Uhlir NJ, Reed JW. 2002. Arabidopsis SHY2/IAA3 inhibits auxin-regulated gene expression. *Plant Cell* **14**: 301–319.

Trewavas A. 2014. *Plant behaviour and intelligence*. Oxford, UK: Oxford University Press.

Tromas A, Perrot-Rechenmann C. 2010. Recent progress in auxin biology. *Comptes Rendus Biologies* **333**: 297–306.

Tsukagoshi H. 2016. Control of root growth and development by reactive oxygen species. *Current Opinion in Plant Biology* **29**: 57–63.

Tsukagoshi H, Busch W, Benfey PN. 2010. Transcriptional regulation of ROS controls transition from proliferation to differentiation in the root. *Cell* **143**: 606–616.

Velasquez SM, Ricardi MM, Dorosz JG, Fernandez PV, Nadra AD, Pol-Fachin L, Egelund J, Gille S, Harholt J, Ciancia M *et al.* 2011. O-Glycosylated cell wall proteins are essential in root hair growth. *Science* **332**: 1401–1403.

Wolf S, Hematy K, Hofte H. 2012. Growth control and cell wall signaling in plants. *Annual Review of Plant Biology* **63**, 381–407.

Xiong J, Yang YJ, Fu GF, Tao LX. 2015. Novel roles of hydrogen peroxide (H_2O_2) in regulating pectin synthesis and demethylesterification in the cell wall of rice (*Oryza sativa)* root tips. *New Phytologist* **206**: 118–126.

Yang J, Cohen Stuart MA, Kamperman M. 2014. Jack of all trades: versatile catechol crosslinking mechanisms. *Chemical Society Reviews* **43**: 8271–8298.

Zhao Y. 2010. Auxin biosynthesis and its role in plant development. *Annual Review of Plant Biology* **61**: 49.

Zhou ZY, Zhang CG, Wu L, Zhang CG, Chai J, Wang M, Jha A, Jia PF, Cui SJ, Yang M *et al.* 2011. Functional characterization of the *CKRC1/TAA1* gene and dissection of hormonal actions in the Arabidopsis root. *Plant Journal* **66**: 516–527.

Supporting Information

Additional Supporting Information may be found online in the Supporting Information tab for this article:

Fig. S1 Treatment with karrikin1 (KAR1) increases *Nicotiana attenuata* seed germination and decreases hypocotyl elongation, but does not induce changes in primary root length.

Fig. S2 Scheme of the meristem zone of *Nicotiana attenuata* roots and longitudinal elongation of cells in the elongation zone induced by smoke.

Fig. S3 Root hair phenotype induced by SPE elutions.

Fig. S4 Root phenotyping in response to different amounts of catechol.

Fig. S5 Comparison of the catechol-induced root phenotype induced by structurally similar di-hydroxy/-methoxy phenolics.

Fig. S6 Hierarchical clustering and functional enrichment analysis of differentially expressed genes (DEGs) in *Nicotiana attenuata* roots after treatment with SPE-fraction S2.

Fig. S7 Real-time auxin response monitoring (DII-VENUS, *Arabidopsis*) indicates increased auxin level after smoke and active fraction S2 incubation within 90 min.

Methods S1 Fractionation of liquid smoke and quantification of catechol.

Table S1 List of differentially expressed genes (DEG) identified by RNAseq.

Please note: Wiley Blackwell are not responsible for the content or functionality of any Supporting Information supplied by the authors. Any queries (other than missing material) should be directed to the *New Phytologist* Central Office.